Transcriptome analysis reveals critical factors for survival after adenovirus serotype 4 infection

Yuhang Zhou,[*,†] Qi Zheng,[*,†] Shipeng Wang,[*,†] Zhouyu Fu,[*,†] Liang Hong,[*,†] Wenjuan Qin,[*,†] Qian Huang,[*,†] Tingting Li,[*,†] Yuhang Zhang,[*,†] Cong Han,[*,†] Daosong Chen,[*,†] Hongquan Chen,[*,†] Martin. F Bachmann,[*,†,‡] Lisha Zha,[*,†,1] and Jian Hao[§]

[*]*College of Animal Science and Technology, Anhui Agricultural University, Hefei 230036, P.R.China;* [†]*International Immunology Centre, Anhui Agricultural University, Hefei 230036, P.R.China;* [‡]*Immunology, RIA, Inselspital, University Hospital Bern, Bern, Switzerland; and* [§]*Shenzhen Jianan Plastic Cosmetic Clinic, Shenzhen, P.R.China*

ABSTRACT Fowl adenovirus serotype-4 (**FAdV-4**) is highly lethal to poultry, making it one of the leading causes of economic losses in the poultry industry. However, a small proportion of poultry can survive after FAdV-4 infection. It is unclear whether there are genetic factors that protect chickens from FAdV-4 infection. Therefore, the livers from chickens uninfected with FAdV-4 (Normal), dead after FAdV-4 infection (Dead) or surviving after FAdV-4 infection (Survivor) were collected for RNA-seq, and 2,649 differentially expressed genes (**DEGs**) were identified. Among these, many immune-related cytokines and chemokines were significantly upregulated in the Dead group compared with the Survivor group, which might indicate that death is related to an excessive inflammatory immune response (cytokine storm). Subsequently, the KEGG results for DEGs specifically expressed in each comparison group indicated that cell cycle and apoptosis-related DEGs were upregulated and metabolism-related DEGs were downregulated in the Dead group, which also validated the reliability of the samples. Furthermore, GO and KEGG results showed DEGs expressed in all three groups were mainly associated with cell cycle. Among them, *BRCA1, CDK1, ODC1*, and *MCM3* were screened as factors that might influence FAdV-4 infection. The qPCR results demonstrated that these 4 factors were not only upregulated in the Dead group but also significantly upregulated in the LMH cells after 24 h infection by FAdV-4. Moreover, interfering with *BRCA1, CDK1, ODC1*, and *MCM3* significantly attenuated viral replication of FAdV-4. And interfering of *BRCA1, CDK1*, and *MCM3* had more substantial hindering effects. These results provided novel insights into the molecular changes following FAdV-4 infection but also shed light on potential factors driving the survival of FAdV-4 infection in chickens.

Key words: fowl adenovirus serotype 4, transcriptome, cytokine storm, infection, RNA-seq

2023 Poultry Science 102:102150
https://doi.org/10.1016/j.psj.2022.102150

INTRODUCTION

Fowl adenovirus serotype-4 (**FAdV-4**) is a highly lethal pathogen, particularly in poultry at the age of 3 to 5 wk with a mortality rate of up to 80% within a week of infection (Asthana et al., 2013; Wang and Zhao, 2019). Its infection is characterized by basophilic intranuclear inclusion bodies, vacuolar degeneration, and multifocal necrosis of hepatocytes, which results in intestinal cachexia (Domanska-Blicharz et al., 2011), hepatitis-pericardial hydrops syndrome (Asthana et al., 2013) and respiratory disease (Dhillon and Kibenge, 1987). The main target of FAdV-4 infection is the liver. So, the mechanisms of molecular changes caused by FAdV-4 infection in the liver are particularly critical (Pan et al., 2017).

Normally, Toll-like receptors (**TLRs**) play major roles in the immune response against DNA viruses. TLR9 senses viral gDNA to promote IFN-α secretion and thus generate antiviral responses. TLR2 and TLR4 recognize certain viral envelope proteins to activate pro-inflammatory cytokines, potentially leading to inflammatory damage (Akira et al., 2006). Currently, the response of Leghorn Male Hepatoma (**LMH**) cell line to FAdV-4 infection is associated with TLR and MAPK signaling pathways (Zhang et al., 2018). In Addition, gene expression levels of certain cytokines (including *TNF-α, IL-6, IFN-γ, IL-1β*, and *IL-12*) and several chemokines (including *IL-8, MIP-1β*, and *MCP-1*) were

Received June 5, 2022.
Accepted August 16, 2022.

[1]Corresponding author: zhalisha@ahau.edu.cn

significantly upregulated in vitro and in vivo resulting from adenovirus infection (Chi et al., 2018; Niu et al., 2018). Transcriptome analysis provides a method to reveal the molecular responses induced by FAdV-4. In recent years, transcriptome changes caused by FAdV-4 is gradually being unraveled, however, these studies are mainly focused on LMH cells after FAdV-4 infection (Zhang et al., 2018), chickens that became symptomatic but did not die after FAdV-4 infection (Chen et al., 2020), or chickens that survived after infection at different times (Ren et al., 2019).

The high pathogenicity of FAdV-4 in chickens causes huge economic losses to farmers, so it is necessary to reveal the critical factors affecting the survival of chickens after FAdV-4 infection To investigate the critical factors for the survival of chickens after FAdV-4 infection, livers from chickens uninfected with FAdV-4, dead after FAdV-4 infection and surviving after FAdV-4 infection were collected for RNA-seq and differentially expressed genes (**DEGs**) were identified. Among them, we focused on DEGs associated with potential cytokine storms after FAdV-4 infection, DEGs that were uniquely expressed in each comparison group, and DEGs that were expressed in all 3 comparison groups. Ultimately, DEGs that might be associated with survival were screened and their effects on FAdV-4 replication were verified in vitro.

MATERIALS AND METHODS

Animals and Ethics Statement

The specific pathogen-free (**SPF**) embryos were purchased from Zhejiang Lihua Agricultural Co., Ltd. (Anhui, China). The birds were kept under healthy extensive care and controlled environmental conditions according to the age and behavior of birds (28−33°C) for 10 d. We tried our best to provide them with a clean and comfortable environment. All birds' care was taken according to the Institutional Animal Care and Use Committee (**IACUS**) guidelines by the school of animal science and technology, Anhui Agricultural University, Hefei, China (**AHAU** 2019-011).

Sample Collection and RNA Extraction

The AH-FAdV-4 strain was obtained from the Anhui Poultry Diagnostic Center (Li et al., 2021). The SPF chicken embryos were used as experimental birds. One hundred and twenty birds hatched from SPF embryos were reared in a sterile environment until 10 d of age and then randomly divided into an infected group and an uninfected group. There were 60 chickens in each group and the 2 groups were kept separately. Chickens in the infected and uninfected groups were treated with 100 μL of AH-FAdV-4 (10^5 $TCID_{50}$) and 100 μL PBS in the intraocular and intranasal mucosa, respectively, following 10 d of observation. The number of chickens that died from FAdV-4 infection was counted. The surviving chickens were subjected to a second challenge (10^5 $TCID_{50}$). All survived birds were euthanized by cervical dislocation. Chicken livers were collected and partially preserved in 4% paraformaldehyde, with the remainder immediately frozen in liquid nitrogen for RNA isolation and viral detection. Livers of chickens that were inoculated with sterile PBS (**Normal**), survived after infection (**Survivor**), and died at 6 d after infection (**Dead**) were selected for the construction of RNA-seq libraries. The Survivor group contained 1 chicken per replicate, and the Normal and Dead groups contained 5 chickens per replicate. Each group had three independent replicates. Total RNA was extracted from three groups of livers using the Trizol kit (Invitrogen, Carlsbad, CA). RNA quality was assessed on an Agilent 2100 Bioanalyzer (Agilent Technologies, Palo Alto, CA) and examined using RNase-free agarose gel electrophoresis.

Section of Liver

The collected livers were fixed in 4% paraformaldehyde for 24 h and then trimmed before being placed in a dehydration cassette. The dehydration boxes were placed in the basket of the dehydrator (JJ-12J, Wuhan Junjie Electronics Co., Ltd., Wuhan, China) and dehydrated with graded alcohol. Subsequently, the completed dehydrated tissues were immersed in paraffin and then embedded in an embedding machine (JB-P5, Wuhan Junjie Electronics Co., Ltd.). The embedded wax blocks were trimmed and placed in the slicer for continuous 4-μm sections. The sections were spread out on warm water at 40°C and dried in an oven at 60°C. All paraffin sections were de-paraffined, followed by dehydration and sealing of the sections.

Polymerase Chain Reaction

Primers for the detection of the AH-FAdV-4 *hexon* gene were designed by Primer-Blast in NCBI and synthesized by Shanghai General Biotech Co., Ltd (Table S1). The Virus Genomic DNA Extraction Kit (TIANGEN, Beijing, China) was used to extract pathogenic DNA according to the instructions. With the extracted DNA as templates, PCR was performed with specific primers of *hexon*. The PCR reaction system (30 μL) comprised 2 μL of template, 15 μL of PCR Nucleotide Mix (10 mmol/L), 11 μL of nuclease-free water, and 1 μL of each of the upstream and downstream primers. The PCR reaction conditions were as follows: pre-denaturation at 94°C for 5 min; denaturation at 94°C for 30 s, annealing at 56°C for 30 s, extension at 72°C for 90 s, 35 cycles; extension at 72°C for a further 10 min. The PCR products were mixed with 6 × DNA loading buffer (MCLAB, South San Francisco, CA) and then electrophoresed using a 1% agarose nucleic acid gel.

Library Construction and Sequencing

All total liver RNA was extracted and the mRNA was subsequently enriched by Oligo (dT) beads. Then, the

enriched mRNA was turned into short fragments using fragmentation buffer and subsequently reverse transcribed into cDNA using random primers. DNA polymerase I, RNase H, dNTP and buffer were used to synthesizing the second strand cDNA. Following purification of the cDNA fragments using the QiaQuick PCR extraction kit (Qiagen, Venlo, the Netherlands), end repair was then performed, poly (A) was added and ligated to the Illumina sequencing adapter. The cDNAs of around 200 bp were screened for PCR amplification using agarose gel electrophoresis and the PCR products were purified again. Sequencing was performed using an Illumina HiSeq2500 (Zhong et al., 2011) from Gene Denovo Biotechnology Ltd (Guangzhou, China).

Bioinformatics Analysis of Nine Libraries

The reads obtained from the sequencer include raw reads containing low-quality bases, which will affect the subsequent assembly and analysis. Hence, reads were further filtered by fastp (Chen et al., 2018) (v0.18.0) to obtain high-quality clean reads (removing low-quality reads containing adapters, unknown nucleotides [N] above 10%, and more than 50% of low quality [Qvalue ≤ 20] bases) (Table S2). Short reads were mapped to the rRNA database using the short reads alignment tool Bowtie2 (Langmead and Salzberg, 2012) (v2.2.8). The rRNA mapped reads were then removed and the remaining reads were further applied for assembly and gene abundance calculation. The index of the reference genome was established and pair-end clean reads were mapped to the reference genome using HISAT (Kim et al., 2015) (v2.2.4) with "-rna-strandness RF". Other parameters were set to default. Mapped reads were assembled for each sample using StringTie v1.3.1 (Pertea et al., 2015, 2016) in a reference-based approach. The read count of each transcript was counted.

Further, fragment per kilobase of transcript per million mapped read (**FPKM**) based on read count was calculated using StringTie to quantify expression abundance and variation. FPKM was able to eliminate the effect of different gene lengths and sequencing data amounts on gene expression calculations. Transcripts with FPKM >2 (at least in one group) were used for subsequent analysis. Principal Component Analysis (**PCA**) of genes was performed with R package models (http://www.r-project.org/). A dead sample was differing from other samples, and it was excluded (Figure S1). Differential expression analysis of genes between 2 different groups was performed using edgeR (Robinson et al., 2010). Genes with false discovery rate (**FDR**) parameters below 0.01 and $|\log2(FC)|\geq2$ were considered as DEGs.

Gene Ontology and Kyoto Encyclopedia of Genes and Genomes

DEGs were mapped to Gene Ontology (**GO**) terms in the Gene Ontology database, gene numbers were calculated for each term, and GO terms that were significantly enriched in DEGs compared to the genome background were defined by hypergeometric tests (Ashburner et al., 2000). Furthermore, KOBAS software was used to test the statistical Kyoto Encyclopedia of Genes and Genomes (**KEGG**) enrichment of genes (Wu et al., 2006). GO and KEGG terms conforming to an FDR <0.05 were defined as significantly enriched.

siRNA-Mediated Silencing of BRCA1, CDK1, ODC1, and MCM3

LMH cells were prepared in 6-well plates with DMEM containing 10% FBS at 37°C in 5% CO_2. Specific siRNA oligonucleotides for *BRCA1, CDK1, ODC1* and *MCM3* were designed using the horizon siDESIGN Center and synthesized by Shanghai General Biotech Co., Ltd (Table S1). Briefly, 5 μL transfection reagent was diluted with 250 μL Opti-MEM for 5 min, while 5 μL siRNA was diluted with 250 μL Opti-MEM. The two mixtures were mixed well and stood for 20 min at room temperature. When LMH cells grow to 50%, removed the medium and added 1.5 mL of culture and 500 μL of the mixture (containing primers and transfection reagent). After 6 h of transfection, a fresh growth medium was replaced and cells were infected with FAdV-4. After 24 h of FAdV-4 infection, RNAs were extracted to identify the expression of 4 candidate genes and DNAs were extracted to identify the *hoxen* gene.

Quantitative Real-Time PCR

The qPCR was performed by 2 × Q3 SYBR qPCR Master mix (TOLOBIO, Shanghai, China) and Real-time Thermal Cycler 5100 (Thermo, Shanghai, China). All the primer pairs were designed using Primer-BLAST in NCBI and synthesized by the Shanghai General Biotech Co., Ltd (Table S1). The *GAPDH* was amplified as a control (Guo et al., 2019). The expression levels of target genes were normalized by *GAPDH*, and $2^{-\Delta\Delta Ct}$ was calculated. The expression of the *hexon* gene of FAdV4 was calculated based on a standard curve, and calculated by $2^{-\Delta Ct}$.

Statistical Analysis

Statistical analysis of the normalized data was then conducted using one-way ANOVA and the least significant difference (**LSD**) in SPSS (v20.0). Expression of 4 candidate genes and *hexon* gene in LMH cells infected with FAdV-4 before and after interference was using Independent Samples *t* test in SPSS. Results were shown as Mean ± SE.

RESULTS

Identification of the Transcriptome in Chicken' Livers

The high lethality of AH-FAdV-4 was illustrated by the fact that 93.33% (56) of 60 chickens died after AH-FAdV-4 infection, with the main mortality occurring 6

Table 1. Mortality of chickens infected with Fadv-4.

	Infection group			Uninfected group		
Days	Number of deaths	Number of survivors	Total number of deaths	Number of deaths	Number of survivors	Total number of deaths
1	0	60	0	0	60	0
2	0	60	0	0	60	0
3	0	60	0	0	60	0
4	0	60	0	0	60	0
5	2	58	2	0	60	0
6	26	32	28	0	60	0
7	24	8	52	0	60	0
8	3	5	55	0	60	0
9	1	4	56	0	60	0
10	0	4	56	0	60	0

to 7 d after the infection (Table 1). All 60 chickens in the uninfected group survived. FAdV-4 *hexon* was present in the livers of all 56 chickens that died in the infected group and was not identified in the 4 survived (10 d after infection) and 60 uninfected chickens, indicating the reliability of the samples (Figure S2). To reveal the transcriptomic changes caused by FAdV-4, RNA-seq was performed on the livers of chickens which uninfected (Normal), died after infection (Dead) and survived after infection (Survivor) (Figure 1A and B). There were 9,443, 9,479 and 9,443 genes (at least FPKM >2 in one group) identified in Normal, Dead, and Survivor groups, respectively (Table S3). Cluster analysis showed the same state of clustering, and the samples in the Normal and Survivor groups were clustered against each other (Figure 1C). The abundance of genes in each group was homogeneous, with higher abundance in the Dead group than in the other 2 groups, suggesting that many genes were upregulated in the livers of chickens after lethal FAdV-4 infection (Figure 1D).

Identification and Analysis of Differentially Expressed Genes

To explore the dynamic changes of gene-expression, we performed differential analysis on the 3 groups. Under stringent filtering conditions ($|\log_2 FC|>2$ and

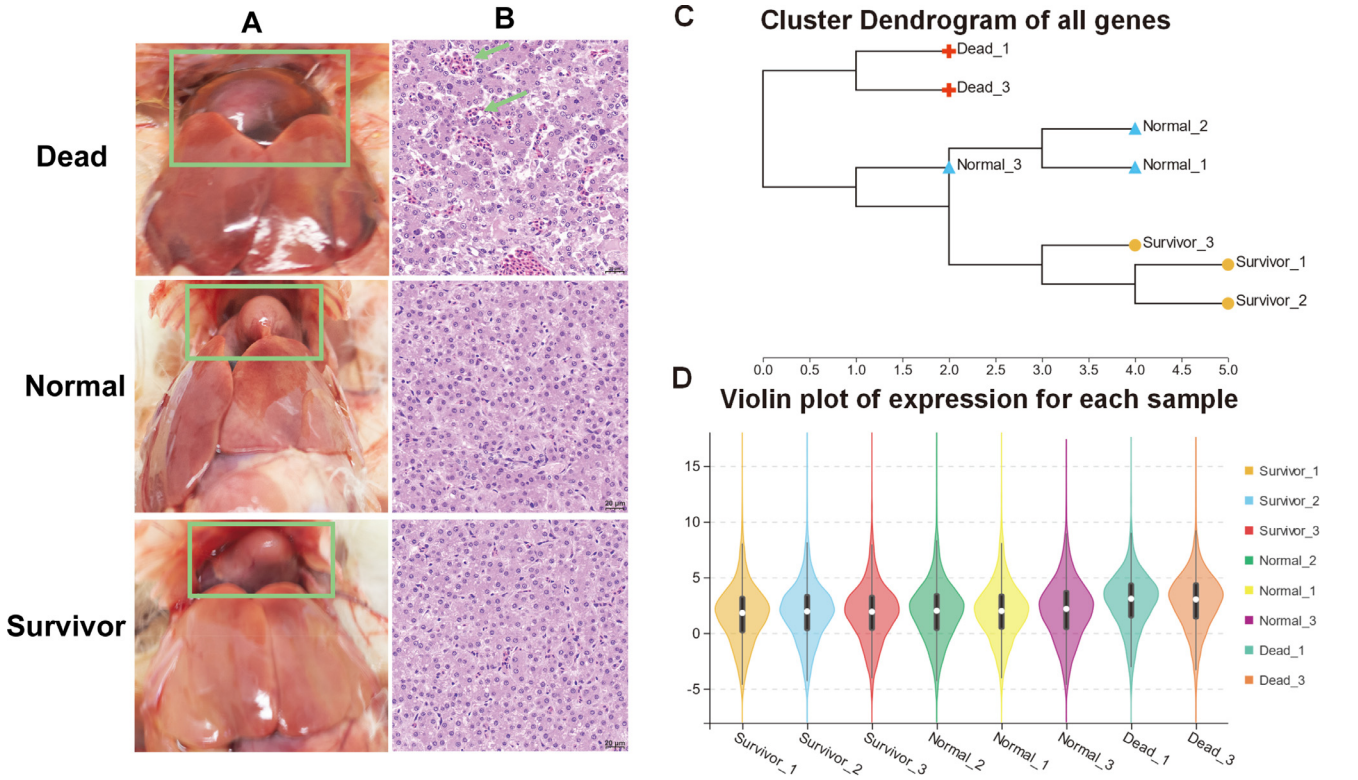

Figure 1. Samples and transcriptome characterization. (A) Chickens in Dead, Survivor, and Normal groups. The green boxes represent the heart. Chickens in the Dead group showed pericardial effusion, while Survivor and Normal groups were healthy. (B) Paraffin sections (hematoxylin-eosin stain, 20 ×) of livers from three groups. The livers of the Normal and Survivor groups were healthy and the Dead group showed significant lesions. (C) Clustering of all genes. (D) Violin plot of expression abundance for each sample. The white dots represent the median; the black rectangles represent the range from the lower quartile (Q1) to the upper quartile (Q3); the outer shapes of the black rectangle represent an estimate of the kernel density. The length of the longitudinal axis represents the degree of dispersion.

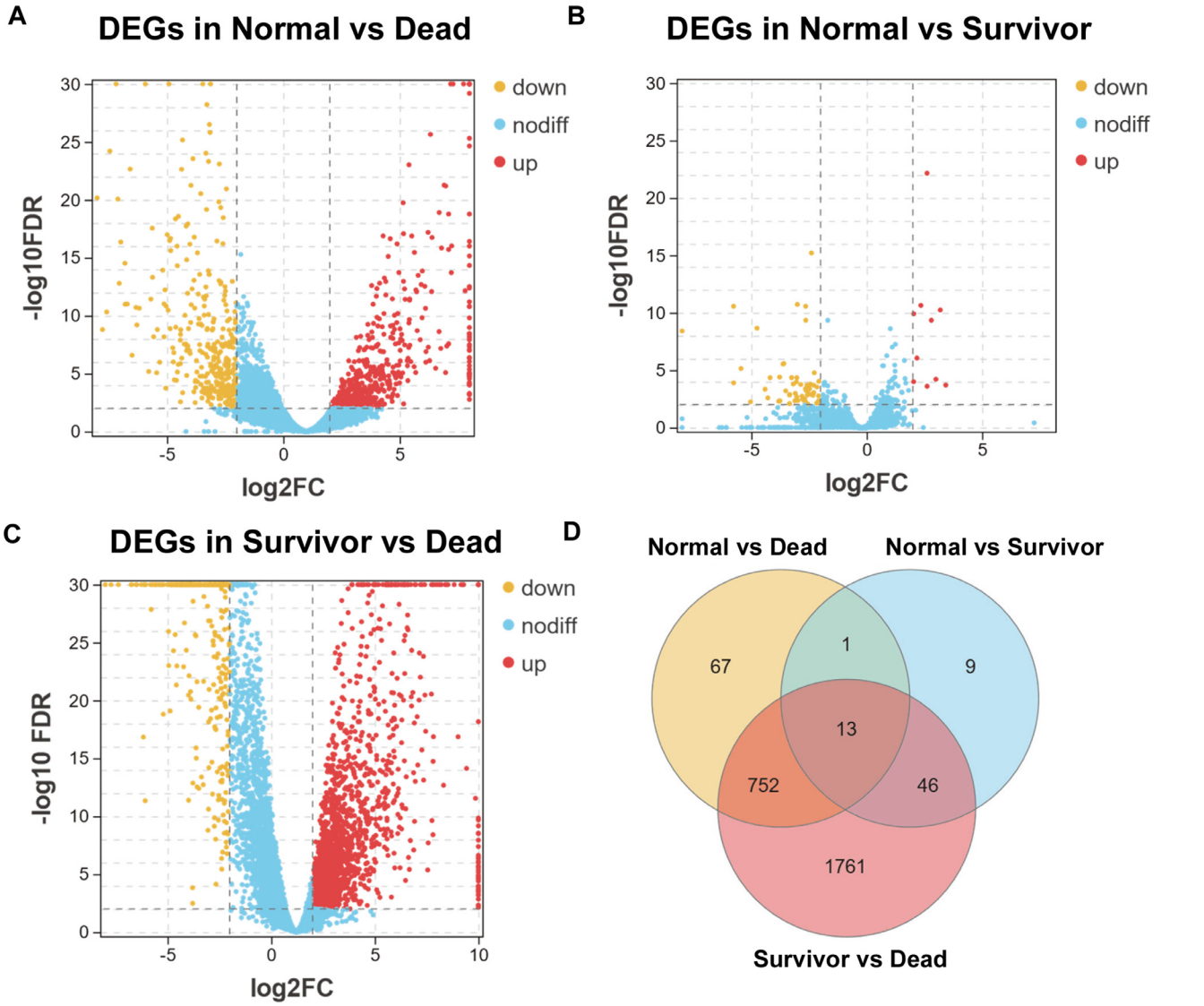

Figure 2. Dynamics of differentially expressed genes in three comparison groups. (A−C) DEGs in Normal vs. Dead group (A), Normal vs. Survivor group (B) and Survivor vs. Dead group (C). Yellow ($log_2FC<-2$) represents downregulated DEGs, red ($log_2FC>2$) represents upregulated DEGs and blue ($-2<log_2FC<2$) represents genes with no differential expression. (D) Venn diagram of DEGs in the three groups. Abbreviation: DEGs, differentially expressed genes

FDR <0.01), 2,649 DEGs were identified (Table S4). Among them, 833 (515 up- and 318 down-regulation), 69 (10 up and 59 down-regulation) and 2,572 (2,234 up- and 338 down-regulation) DEGs were found in the Normal vs. Dead, Normal vs. Survivor and Survivor vs. Dead comparison groups, respectively (Figures 2A−2C). Interestingly, a few DEGs were found in the Normal vs. Survivor group, but a much larger number of DEGs was found in the Survivor vs. Dead group. Among them, immune-related cytokines and chemokines were significantly upregulated in the Dead group compared to the Normal group except for IL-15 (Figure S3). Whereas they did not differ in the Normal and Survivor groups. Additionally, the Venn diagram showed that there were 9, 67 and 1,761 DEGs uniquely expressed in Normal vs Survivor, Normal vs. Dead and Survivor vs. Dead groups, respectively, and 13 DEGs were expressed in all 3 groups (Figure 2D). These unique and shared DEGs were focused on in the following analysis.

Differentially Expressed Genes Uniquely Expressed in Each Comparison Group

These uniquely expressed DEGs in different comparison groups might represent the onset/termination of specific physiological processes following FAdV-4 infestation. Hence, uniquely expressed DEGs in each group were selected for KEGG analysis. There were 1,761 DEGs between the Survivor and Dead, with only 73 downregulated, and 1,688 upregulated (Figure 3A). The upregulated DEGs were enriched to 27 KEGG terms, mainly including "Proteasome", "Spliceosome", "Cell cycle" etc., with apoptosis being the most associated with other pathways (Figures 3B and 3C, Table S5). The downregulated DEGs were mainly enriched in 5 metabolism-related pathways, with the "Metabolic pathways" in a hub position (Figures 3D and 3E, Table S5). These were characteristic of death following FAdV-4 infection, as shown by reduced metabolism,

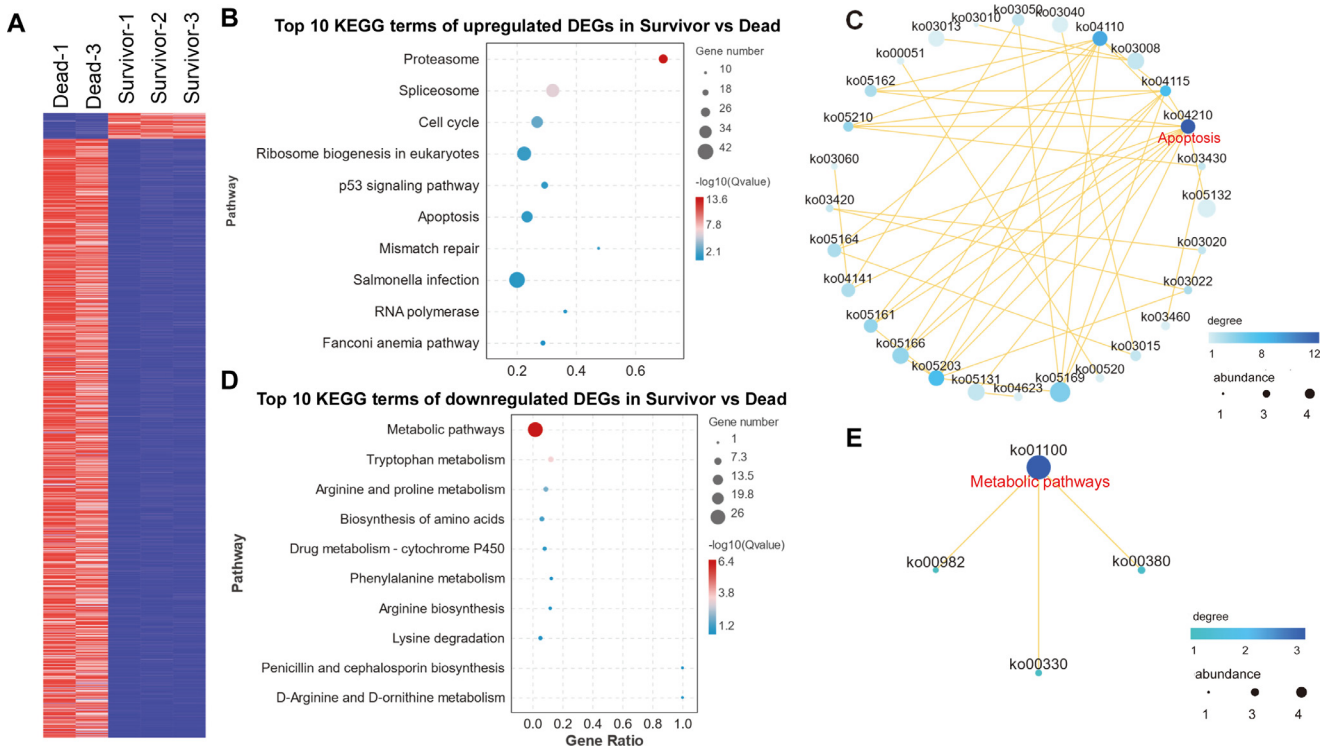

Figure 3. Analysis of uniquely differentially expressed genes in the survivor vs. dead group. (A) Heatmap of all DEGs uniquely expressed in the Survivor vs. Dead group. The color represents abundance. (B and D) Top 10 KEGG terms of upregulated (B) and downregulated (D) DEGs in Survivor vs. Dead group. The size of the bubble represents the number of DEGs. The color represents *Q*value (FDR). (C and E) The networks of upregulated (C) and downregulated (E) DEGs in the Survivor vs. Dead group. Color represents degrees. Size represents abundance. The pathways with the most degrees are shown in the figure. Abbreviations: DEGs, differentially expressed genes; FDR, false discovery rate.

increased replication, and apoptosis. Consistent with the previous group, the DEGs between Normal and Dead were mainly enriched in "Metabolic pathways", which were linked to "Drug metabolism - cytochrome P450", "Drug metabolism - other enzymes" and "Biosynthesis of unsaturated fatty acids" (Figure S4A, Table S5). There were 21 DEGs enriched in "Metabolic pathways", but only AK1 was upregulated in the Dead group, probably caused by the loss of active metabolism shortly after death (Figure 4B). There were only 9 DEGs between Normal and Survivor, and they were involved in 9 pathways, 7 of which were associated with metabolism (Figures 4C and 4D).

Differentially Expressed Genes Expressed in Three Comparison Groups

If there are critical factors in survivors, they need to be differentially expressed in all 3 groups (Figure S5A). GO and KEGG analyses were performed on the 13 DEGs expressed in all 3 groups. GO analysis enriched 176 terms, mostly related to various stages of the cell cycle (Figure 4A, Table S6). KEGG was enriched for only one term of the cell cycle (Figure 4B, Table S6). The screening of critical DEGs was subject to the assumptions of Figure S5A. The 12 DEGs that fulfilled the assumption were selected for qPCR validation (Figures S5B–D). QPCR results for *CDC45, BRCA1, CDK1, KIF23, ODC1, MCM3, SKA3, UPP2, ENSGALG00000045842,* and *NCAPH2* were consistent with RNA-seq and were differentially expressed in the comparison groups (Figure 5). *UBE2C* was highly expressed in the Dead group but not differentially in the Normal and Survivor groups. *GLDC* was downregulated in the Dead group but not differentially in the Normal and Survivor groups.

Interference with BRCA1, CDK1, ODC1, and MCM3 Blocks FAdV-4 Replication

BRCA1, CDK1, ODC1, and *MCM3* associated with the viral disease were explored as critical candidates for survival. *BRCA1* ($P = 0.006$), *CDK1* ($P = 0.007$), *ODC1* ($P < 0.001$), and *MCM3* ($P = 0.013$) were both upregulated in LMH cells after FAdV-4 infection (Figure 6A). Then, they were successfully silenced in LHM cells, respectively (Figure 6B). After interference with these 4 DEGs, FAdV-4 replication was inhibited by *ODC1* ($P = 0.029$), and significantly inhibited by the *BRCA1* ($P < 0.001$), *CDK1* ($P < 0.001$) and *MCM3* ($P < 0.001$; Figures 6C–6F). Thus, *BRCA1, CDK1,* and *MCM3* may be involved in increased birds' susceptibility to FAdV-4 infection.

DISCUSSION

FAdV-4 is a highly lethal hepatophilic virus with the liver as its main target organ (Pan et al., 2017; Wang and Zhao, 2019). Most chickens infected with FAdV-4 will die acutely, the surviving chickens have stunted

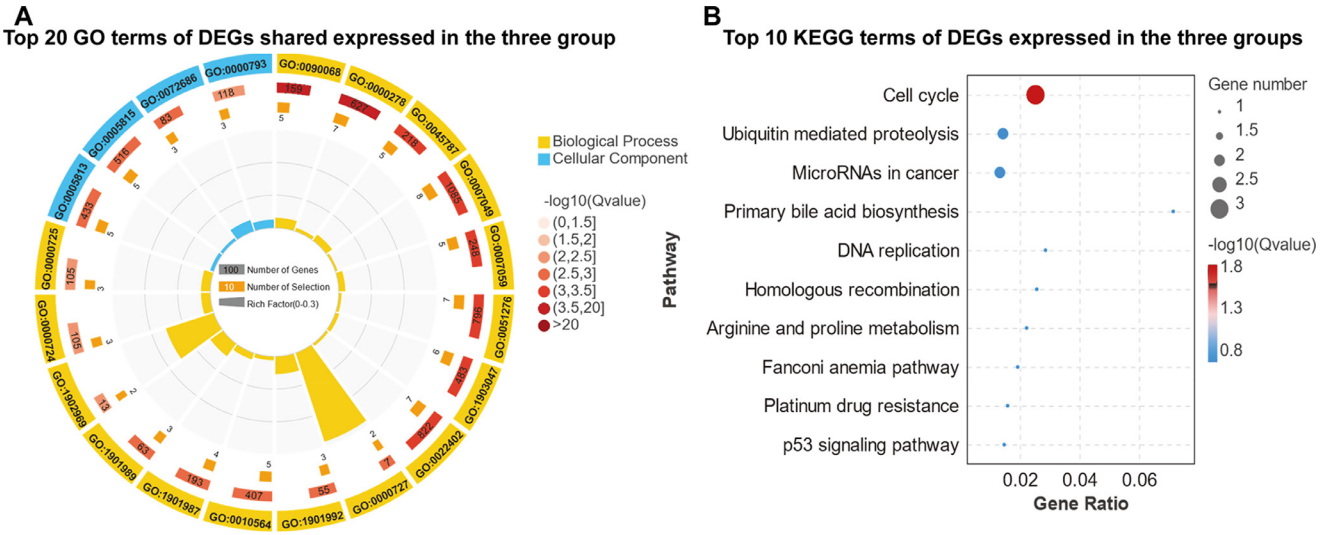

Figure 4. GO and KEGG analyses of differentially expressed genes expressed in all three groups (A) Circle diagram of the top 20 GO-enriched terms for DEGs expressed in all 3 groups. First circle: the top 20 enriched GO terms, different colors represent different Ontologies. Blue represents cellular component, yellow represents biological process. Second circle: the number of background genes of this GO term and the FDR. The more genes the longer the bar, the smaller the FDR the redder the color. Third circle: the number of DEGs enriched to the corresponding GO term. Fourth circle: Rich Factor values for each GO term. (B) Top 10 KEGG terms of DEGs expressed in all 3 groups. The size of the bubble represents the number of DEGs. The color represents FDR. Abbreviations: DEGs, differentially expressed genes; FDR, false discovery rate; GO, gene ontology; KEGG, Kyoto Encyclopedia of Genes and Genomes.

growth, suppressed humoral immunity, and increased incidence of respiratory disease (Niu et al., 2017). Thus, it is important to explore the genetic changes in the host livers after FAdV-4 infection. RNA-seq has become an essential tool to reveal the genetic changes. Normally, FPKM and TPM are methods to measure the expression of a gene. In the FPKM method[1], the number of Fragments of a gene is first divided by the length of the gene, and the ratio is then divided by the total exon length of all genes. TPM[2] is the ratio of gene's FPKM divided by the sum of FPKM multiplied by 10^6. Both FPKM (Xing et al., 2020) and TPM (Wu et al., 2019) are widely used for the observation of gene expression trends, from which, we chose FPKM to perform gene expression. RNA-seq has been used to identify DEGs in the livers of chickens (10 d) that survived at 7, 14, and 21 d after FAdV-4 infection. These DEGs were identified to be involved in the biological processes of PPAR and Notch signaling, and the signaling pathways of cytokine-cytokine receptor interactions and Toll-like receptors (Ren et al., 2019). Besides, Chen et al. (2020) explored transcriptomic changes in the livers of chickens (40 d) infected with FAdV-4 for 2 d, focusing on the DEGs in the phagosome pathway. Among them, *F-actin, Rab7, TUBA,* and *DVnein* were screened as key factors for FAdV-4 invasion and movement within the LMH cells in vitro. In this study, we focused on transcriptomic changes in the livers of chickens (10 d) that were inoculated with sterile PBS (Normal), survived after FAdV-4 infection (Survivor), and died at 6 d after FAdV-4 infection (Dead). Subsequently, the genes involved in a potential "cytokine storm", and the pathways involved by DEGs specifically expressed in each group and the effects of DEGs expressed in all 3 groups on FAdV-4 replication were specifically studied.

Aggressive inflammation, also known as "cytokine storm", is a life-threatening systemic inflammatory syndrome associated with uncontrolled pro-inflammatory responses (Yang and Tang, 2016, Karki and Kanneganti, 2021). In influenza virus-related studies, increased viral load causes excessive activation of epithelial cells and platelets, which induce excessive pro-inflammatory cytokine expression. These excessive-inflammatory responses lead to fatal multi-organ failure and hyperacute mortality in chickens (Yang and Tang, 2016; Mishra et al., 2017). Therefore, dysregulation of the innate immune response might be a critical determinant of the severity and outcome of viral infection. High expression of cytokines (*IFNA, IFNG, IL-1, IL-6, IL-12, IL-10, IL-18*, and *TNF-α*) and chemokines (*CCL2, CCL4, CCL5* and *CXCL10*) following influenza virus infection has been reported to cause tissue damage and high mortality in chickens as well as other animals (Mishra et al., 2017). After 3 to 5 d of FAdV-4 infection, cytokines were upregulated along with hemorrhage and congestion, indicating consistent clinical symptoms and cytokine changes (Wu et al., 2020). However, the full extent and mechanism of the "cytokine storm" caused by FAdV-4 remains unclear. So, we first focused on DEGs related to the innate immune response against FAdV-4 infection, such as IL factors (*IL-6, IL-12β, IL-1β, IL-18, IL-8, IL-15*, and *IL-16*), TLR-related factors (*TLR1β* and *TLR15*), chemokines (*CCL4, CCL5, CCL21*, and *CCL19*), which were significantly upregulated in the Dead group. Meanwhile, the receptor for IFNα (*IFNAR1*), the receptors for IL (*IL13RA1, IL10RA,*

[1]$\text{FPKM} = \frac{\text{Gene's exon fragment}}{\text{Mapped reads (Millions)} \times \text{Exon length (KB)}}$

$\text{TPM} = \frac{\text{Gene's FPKM}}{\text{sum(total FPKM)}} \times 10\text{^}6$

[2]$\text{TPM} = \frac{\text{Gene's FPKM}}{\text{sum(total FPKM)}} \times 10\text{^}6$

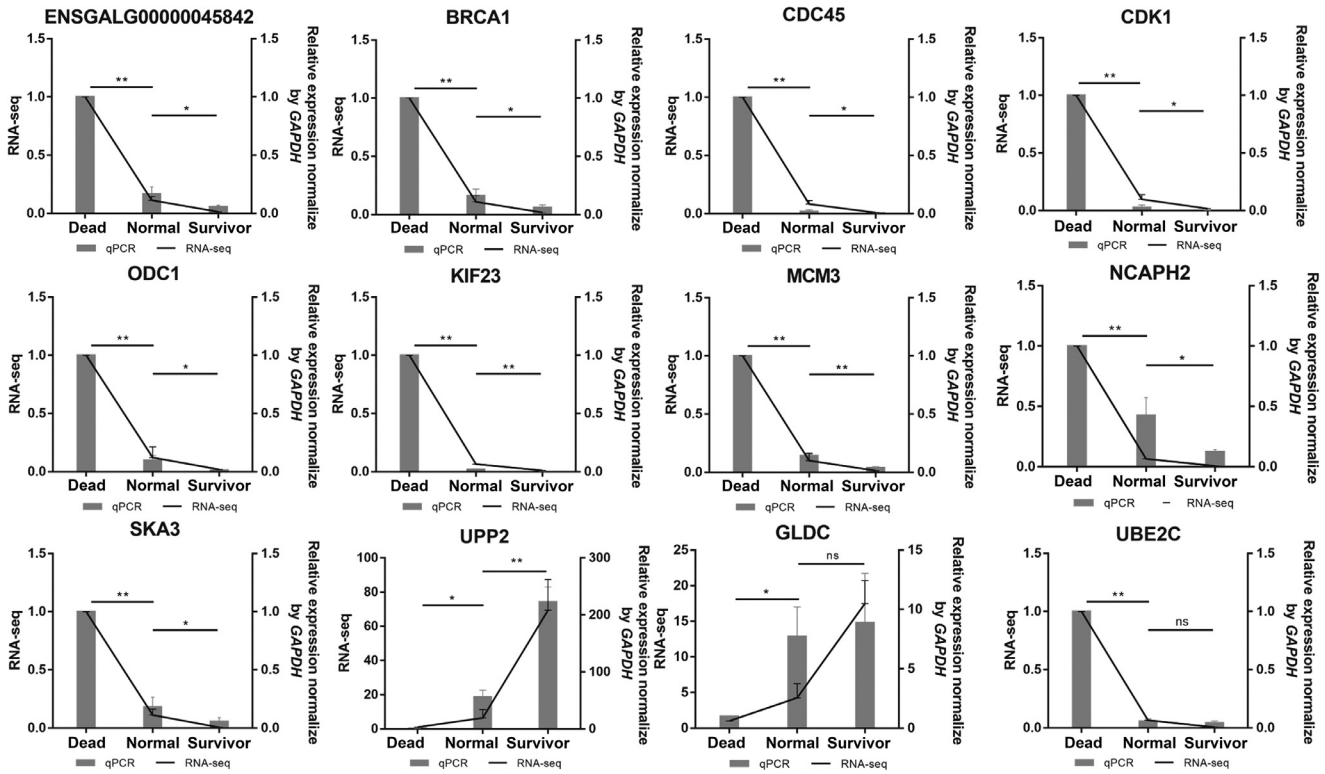

Figure 5. QPCR validation of 12 candidated differentially expressed genes. The qPCR (Bar chart, orange) and RNA-seq expression (Line chart, blue) validation of the 12 candidate DEGs. "**" represents a significant difference ($P < 0.01$); "*" represents a difference ($P < 0.05$); "ns" represents no difference ($P > 0.05$).

IL10RB, IL17RA, IL-21R, IL1R2, IL1RL1, IL22RA1, and *IL7R*), the receptors for TNF (*TNFRSF10B, TNFRSF11B, TNFRSF1A TNFRSF4, TNFRSF6B*, and *TNFRSF9*), and the factors they induced (*TNFAIP3, IL4I1*, and *IL8L1*), also showed upregulation. This study characterized at the molecular level "cytokine storm" that may occur following FAdV-4 infection.

In addition, DEGs specifically expressed in each group and expressed in all 3 groups were also noted. The DEGs specifically expressed in each group may represent the onset/termination of specific physiological processes following FAdV-4 infestation. DEGs in the Dead group were consistent with features of death, such as reduced metabolism and apoptosis. Meanwhile, the increased expression of proliferation-associated DEGs implied that immune cells may have generated a strong response prior to death. The 9 uniquely expressed DEGs between the Normal and Survivor groups were involved in 7 pathways that related to metabolism, such as "Cysteine and methionine metabolism", "Glutathione metabolism and Steroid biosynthesis". Metabolomic analysis of FAdV-4-infected LMH cells also highlights the importance of host cell metabolism in viral replication (Ma and Niu, 2021).

As 6.67% of the chickens in this study survived the infection, it is hypothesized that there are factors in the target organs that help the survived chickens to resist or hinder FAdV-4 infestation. At the same time, these factors need to be differentially expressed in all 3 comparison groups (Figure S5A). This assumption was satisfied by 12 of 13 DEGs from the 3 groups, which were enriched in cell cycle-related terms. For example, the CDC45 protein has been reported to have a central role in the cell cycle and in the initiation and prolongation of chromosomal DNA replication in eukaryotic cells in response to DNA damage (Broderick and Nasheuer, 2009). The activation and catalytic ubiquitination activity of UBE2C is part of the response mechanism that ensures accurate sister chromatid segregation (Yamaguchi et al., 2016). Moreover, the pro-proliferative and cell cycle-regulating effects of *NCAPH2* (Wallace et al., 2019), *KIF23* (Fischer et al., 2016), *GLDC* (Alptekin et al., 2019), *SAK3* (Tang et al., 2021) on other cells have also been described.

Interestingly, 5 of these DEGs were associated with infection by other viruses as well. Among these, *GLDC* has been shown to have antiviral effects in avian influenza, but its antiviral modality is based on the amplification of type I IFN and interferon−stimulated genes (Zhou et al., 2019a). This might have contributed to the development of the "cytokine storm". Further, BRCA1, an essential protein for maintaining chromosomal stability, is also pivotal in the proteome of chicken lungs after avian influenza virus infection (Yoshida and Miki, 2004; Vijayakumar et al., 2022). CDK1 regulates the G2 phase of chicken DT40 cells and is the essential target protein for Marek's Disease Virus (Zhou et al., 2019b; Samejima et al., 2022). ODC1, which has been reported to be pro-proliferative in a variety of cells, is also upregulated following Porcine epidemic diarrhea virus infection (Ye et al., 2019; Xie et al., 2022). Moreover, MCM3, which is

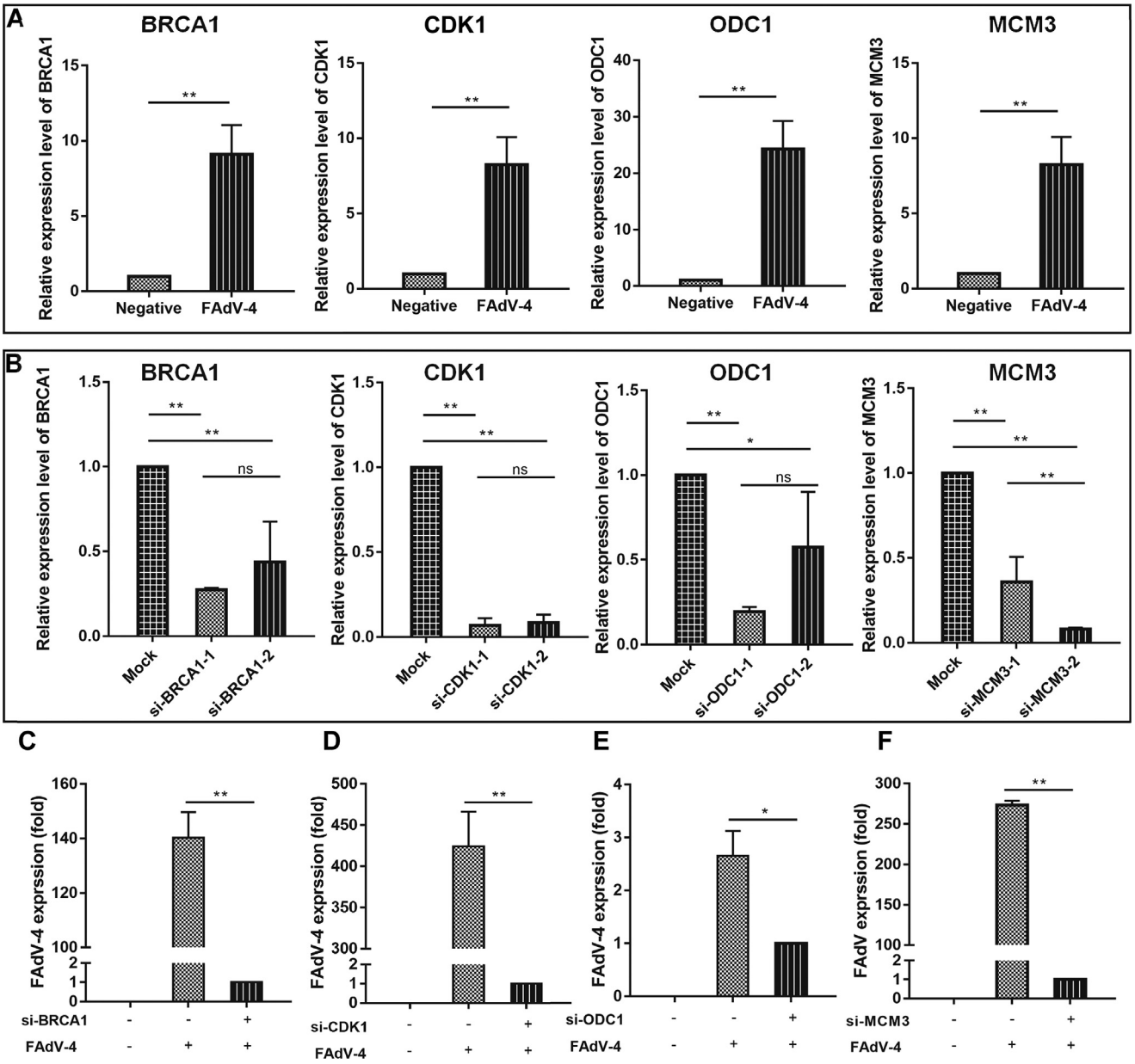

Figure 6. Effects of interfering with four candidates on FAdV-4 replication. (A) Expression levels of *BRCA1, CDK1, ODC1,* and *MCM3* in normal and infected LMH cells. (B) Expression levels of *BRCA1, CDK1, ODC1,* and *MCM3* in LMH cells after interfering. (C–F) Replication of FAdV-4 after interference with *BRCA1, CDK1, ODC1,* and *MCM3* in LMH cells. "**" represents a significant difference ($P < 0.01$); "*" represents a difference ($P < 0.05$); "ns" represents no difference ($P > 0.05$).

crucial to the maintenance of the MCM2-7 hexamer in DNA replication, is also an important candidate for avian influenza virus-host interactions (Wang et al., 2016; Saito et al., 2022). *BRCA1, CDK1, ODC1*, and *MCM3* but not GLDC were selected as survival candidates for validation due to inconsistency between qPCR and RNA-seq of *GLDC*. The results showed that interference with these 4 genes downregulated FAdV-4 replication and that replication was most downregulated by *BRCA1, CDK1* and *MCM3*.

While this study screened for critical factors that associated with survival after FAdV-4 infection based on the transcriptome, this is not the full landscape of the epigenetics of FAdV-4 infection. Epigenetics encompasses multiple Omics, such as genome, proteome, DNA methylation, whole transcriptome, etc. Combining multiple Omics to explore the epigenetics after FAdV-4 infection and identify critical factors will provide novel perspectives.

ACKNOWLEDGMENTS

We would like to acknowledge Prof. Fangfang Chen who provided the FAdV-4 strain. This work was supported by projects from Anhui Agricultural University: The Rewards, Subsidies and Platform Support for Talent Introduction [grant number rc392006] and Animal Molecule and Applied Immune Innovation Team [grant number 03082136]

Author contributions: Yuhang Zhou conceived and designed the research. Lisha Zha provided acquisition of the financial support for the project leading to this

publication. Qi Zheng performed the analysis of data. Yuhang Zhou, Shipeng Wang, Zhouyu Fu, Qian Huang and Liang Hong conducted experiments. Qi Zheng, Wenjuan Qin, Tingting Li, Yuhang Zhang and Cong Han wrote the manuscript. Daosong Chen, Hongquan Chen, Bachmann Martin, Lisha Zha and Jian Hao revised the manuscript. All authors read and approved the manuscript.

DISCLOSURES

The authors declare that they have no known competing financial interests or personal relationships that could have appeared to influence the work reported in this paper.

SUPPLEMENTARY MATERIALS

Supplementary material associated with this article can be found, in the online version, at doi:10.1016/j.psj.2022.102150.

REFERENCES

Akira, S., S. Uematsu, and O. Takeuchi. 2006. Pathogen recognition and innate immunity. Cell. 124:783–801.

Alptekin, A., B. Ye, Y. Yu, C. Poole, J. van Riggelen, Y. Zha, and H. F. Ding. 2019. Glycine decarboxylase is a transcriptional target of MYCN required for neuroblastoma cell proliferation and tumorigenicity. Oncogene. 38:7504–7520.

Ashburner, M., C. Ball, J. Blake, D. Botstein, H. Butler, J. M. Cherry, A. P. Davis, K. Dolinski, S. S. Dwight, J. T. Eppig, M. A. Harris, D. P. Hill, L. Issel-Tarver, A. Kasarskis, S. Lewis, J. C. Matese, J. E. Richardson, M. Ringwald, G. M. Rubin, and G. Sherlock. 2000. Gene ontology: tool for the unification of biology. The Gene Ontology Consortium. Nat. Genet. 25:25–29.

Asthana, M., R. Chandra, and R. Kumar. 2013. Hydropericardium syndrome: current state and future developments. Arch. Virolo. 158:921–931.

Broderick, R., and H. Nasheuer. 2009. Regulation of Cdc45 in the cell cycle and after DNA damage. Biochem. Soc. T. 37:926–930.

Chen, S., Y. Zhou, Y. Chen, and J. Gu. 2018. fastp: an ultra-fast all-in-one FASTQ preprocessor. Bioinformatics. 34:i884–i890.

Chen, Y., R. Huang, G. Qu, Y. Peng, L. Xu, C. Wang, C. Huang, and Q. Wang. 2020. Transcriptome analysis reveals new insight of fowl adenovirus serotype 4 infection. Front. Microbiol. 11:146.

Chi, G., X. Feng, Y. Ru, T. Xiong, Y. Gao, H. Wang, Z. L. Luo, R. Mo, F. Guo, Y. P. He, G. M. Zhang, D. A. Tian, and Z. H. Feng. 2018. TLR2/4 ligand-amplified liver inflammation promotes initiation of autoimmune hepatitis due to sustained IL-6/IL-12/IL-4/IL-25 expression. Mol. Iimmunol. 99:171–181.

Dhillon, A., and F. Kibenge. 1987. Adenovirus infection associated with respiratory disease in commercial chickens. Avian. Dis. 31:654–657.

Domanska-Blicharz, K., G. Tomczyk, K. Smietanka, W. Kozaczynski, and Z. Minta. 2011. Molecular characterization of fowl adenoviruses isolated from chickens with gizzard erosions. Poult. Sci. 90:983–989.

Fischer, M., M. Quaas, L. Steiner, and K. Engeland. 2016. The p53-p21-DREAM-CDE/CHR pathway regulates G2/M cell cycle genes. Nucleic. Acids. Res. 44:164–174.

Guo, X., J. X Wang, H. Chen, H. Su, Z. C. Wang, Y. Wan, Y. Y. Huang, and R. S. Jiang. 2019. Effects of exercise on carcass composition, meat quality, and mRNA expression profiles in breast muscle of a Chinese indigenous chicken breed. Poult. Sci. 98:5241–5246.

Karki, R., and T. Kanneganti. 2021. The 'cytokine storm': molecular mechanisms and therapeutic prospects. Trends. Immunol. 42:681–705.

Kim, D., B. Langmead, and S. Salzberg. 2015. HISAT: a fast spliced aligner with low memory requirements. Nat. Methods. 12:357–360.

Langmead, B., and S. Salzberg. 2012. Fast gapped-read alignment with Bowtie 2. Nat. Methods. 9:357–359.

Li, M., M. Raheem, C. Han, F. Yu, Y. Dai, M. Imran, Q. Hong, J. Zhang, Y. Tan, L. Zha, and F. Chen. 2021. The fowl adenovirus serotype 4 (FAdV-4) induce cellular pathway in chickens to produce interferon and antigen-presented molecules (MHCI/II). Poult. Sci. 100:101406.

Ma, H., and Y. Niu. 2021. Metabolomic profiling reveals new insight of fowl adenovirus serotype 4 infection. Front. Microbiol. 12:784745.

Mishra, A., P. Vijayakumar, and A. Raut. 2017. Emerging avian influenza infections: current understanding of innate immune response and molecular pathogenesis. Int. Rev. Immunol. 36:89–107.

Niu, Y., Q. Sun, G. Zhang, X. Liu, Y. Shang, Y. Xiao, and S. Liu. 2018. Fowl adenovirus serotype 4-induced apoptosis, autophagy, and a severe inflammatory response in liver. Vet. Microbiol. 223:34–41.

Niu, Y., Q. Sun, G. Zhang, W. Sun, X. Liu, Y. Xiao, Y. Shang, and S. Liu. 2017. Pathogenicity and immunosuppressive potential of fowl adenovirus in specific pathogen free chickens. Poultry. Sci. 96:3885–3892.

Pan, Q., Y. Yang, Z. Shi, L. Liu, Y. Gao, X. Qi, C. Liu, Y. Zhang, H. Cui, and X. Wang. 2017. Different dynamic distribution in chickens and ducks of the hypervirulent, novel genotype fowl adenovirus serotype 4 recently emerged in China. Front. Microbiol. 8:1005.

Pertea, M., D. Kim, G. M. Pertea, J. T. Leek, and S. L. Salzberg. 2016. Transcript-level expression analysis of RNA-seq experiments with HISAT, StringTie and Ballgown. Nat. Protoc. 11:1650–1667.

Pertea, M., G. M. Pertea, C. M. Antonescu, T. C. Chang, J. T. Mendell, and S. L. Salzberg. 2015. StringTie enables improved reconstruction of a transcriptome from RNA-seq reads. Nat. Biotechnol. 33:290–295.

Ren, G., H. Wang, M. Huang, Y. Yan, F. Liu, and R. Chen. 2019. Transcriptome analysis of fowl adenovirus serotype 4 infection in chickens. Virus. Genes. 55:619–629.

Robinson, M., D. McCarthy, and G. Smyth. 2010. edgeR: a Bioconductor package for differential expression analysis of digital gene expression data. Bioinformatics. 26:139–140.

Saito, Y., V. Santosa, K. Ishiguro, and M. Kanemaki. 2022. MCMBP promotes the assembly of the MCM2-7 hetero-hexamer to ensure robust DNA replication in human cells. eLife. 11:e77393.

Samejima, I., C. Spanos, K. Samejima, J. Rappsilber, G. Kustatscher, and W. Earnshaw. 2022. Mapping the invisible chromatin transactions of prophase chromosome remodeling. Mol. Cell. 82:696–708 e694.

Tang, J., J. Liu, J. Li, Z. Liang, K. Zeng, H. Li, Z. Zhao, L. Zhou, and N. Jiang. 2021. Upregulation of SKA3 enhances cell proliferation and correlates with poor prognosis in hepatocellular carcinoma. Oncol. Rep. 45:48.

Vijayakumar, P., A. Raut, S. Chingtham, H. Murugkar, D. Kulkarni, R. Sood, V. P. Singh, and A. Mishra. 2022. Proteomic analysis of differential expression of lung proteins in response to highly pathogenic avian influenza virus infection in chickens. Arch. Virol. 167:141–152.

Wallace, H., V. Rana, H. Nguyen, and G. Bosco. 2019. Condensin II subunit NCAPH2 associates with shelterin protein TRF1 and is required for telomere stability. J. Cell. Pysiol. 234:20755–20768.

Wang, Q., Q. Li, R. Liu, M. Zheng, J. Wen, and G. Zhao. 2016. Host cell interactome of PA protein of H5N1 influenza A virus in chicken cells. J. Proteomics. 136:48–54.

Wang, Z., and J. Zhao. 2019. Pathogenesis of hypervirulent fowl adenovirus serotype 4: the contributions of viral and host factors. Viruses. 11:741.

Wu, J., X. Mao, T. Cai, J. Luo, and L. Wei. 2006. KOBAS server: a web-based platform for automated annotation and pathway identification. Nucleic. Acids. Res. 1:34.

Wu, N., B. Yang, B. Wen, W. Li, J. Guo, X. Qi, Y. Shang, and S. Liu. 2020. Pathogenicity and immune responses in specific-pathogen-free chickens during fowl adenovirus serotype 4 infection. Avian. Dis. 64:315–323.

Wu, Z., L. Ding, J. Bao, Y. Liu, Q. Zhang, J. Wang, R. Li, M. Ishfaq, and J. Li. 2019. Co-infection of Mycoplasma gallisepticum and Escherichia coli Triggers Inflammatory Injury Involving the IL-17 Signaling Pathway. Front. Microbiol. 10:2615.

Xie, H., Q. Ai, T. Tong, M. Liao, and H. Fan. 2022. PEDV infection affects the expression of polyamine-related genes inhibiting viral proliferation. Virus. Res. 312:198708.

Xing, Q. R., C. A. El Farran, P. Gautam, Y. S. Chuah, T. Warrier, C. D. Toh, N. Y. Kang, S. Sugii, Y. T. Chang, J. Xu, J. J. Collins, G. Q. Daley, H. Li, L. F. Zhang, and Y. H. Loh. 2020. Diversification of reprogramming trajectories revealed by parallel single-cell transcriptome and chromatin accessibility sequencing. Sci. Adv. 6: eaba1190.

Yamaguchi, M., R. VanderLinden, F. Weissmann, R. Qiao, P. Dube, N. Brown, D. Haselbach, W. Zhang, S. S. Sidhu, J. M. Peters, H. Stark, and B. A. Schulman. 2016. Cryo-EM of mitotic checkpoint complex-bound APC/C reveals reciprocal and conformational regulation of ubiquitin ligation. Mol. Cell. 63:593–607.

Yang, Y., and H. Tang. 2016. Aberrant coagulation causes a hyper-inflammatory response in severe influenza pneumonia. Cell. Mol. Immunol. 13:432–442.

Ye, Z., Z. Zeng, Y. Shen, Q. Yang, D. Chen, Z. Chen, and S. Shen. 2019. ODC1 promotes proliferation and mobility via the AKT/GSK3β/β-catenin pathway and modulation of acidotic microenvironment in human hepatocellular carcinoma. OncoTargets. Ther. 12:4081–4092.

Yoshida, K., and Y. Miki. 2004. Role of BRCA1 and BRCA2 as regulators of DNA repair, transcription, and cell cycle in response to DNA damage. Cancer Sci. 95:866–871.

Zhang, J., Z. Zou, K. Huang, X. Lin, H. Chen, and M. Jin. 2018. Insights into leghorn male hepatocellular cells response to fowl adenovirus serotype 4 infection by transcriptome analysis. Vet. Microbiol. 214:65–74.

Zhong, S., JG. Joung, Y. Zheng, YR. Chen, B. Liu, Y. Shao, JZ. Xiang, Z. Fei, and JJ. Giovannoni. 2011. High-throughput illumina strand-specific RNA sequencing library preparation. Cold. Spring. Harb. Protoc. 1:940–949.

Zhou, J., D. Wang, B. Wong, C. Li, V. Poon, L. Wen, X. Zhao, M. C. Chiu, X. Liu, Z. Ye, S. Yuan, K. H. Sze, J. F. Chan, H. Chu, K. K. To, and K. Y. Yuen. 2019. Identification and characterization of GLDC as host susceptibility gene to severe influenza. EMBO. Mol. Med. 11:e9528.

Zhou, X., S. Wu, H. Zhou, M. Wang, M. Wang, Y. Lü, Z. Cheng, J. Xu, and Y. Ai. 2019. Marek's disease virus regulates the ubiquitylome of chicken CD4 T cells to promote tumorigenesis. Int. J. Mol. Sci. 20:2089.